Kong *et al.*
Acta Neuropathologica Communications (2023) 11:65
https://doi.org/10.1186/s40478-023-01537-6

Acta Neuropathologica Communications

RESEARCH

Open Access

The locus coeruleus input to the rostral ventromedial medulla mediates stress-induced colorectal visceral pain

Dexu Kong[1,2†], Yunchun Zhang[1,2†], Po Gao[1,2†], Chao Pan[1,2], Haoyue Deng[1,2], Saihong Xu[1,2], Dan Tang[1,2], Jie Xiao[1,2], Yingfu Jiao[1,2*], Weifeng Yu[1,2*] and Daxiang Wen[1,2*]

Abstract

Unlike physiological stress, which carries survival value, pathological stress is widespread in modern society and acts as a main risk factor for visceral pain. As the main stress-responsive nucleus in the brain, the locus coeruleus (LC) has been previously shown to drive pain alleviation through direct descending projections to the spinal cord, but whether and how the LC mediates pathological stress-induced visceral pain remains unclear. Here, we identified a direct circuit projection from LC noradrenergic neurons to the rostral ventromedial medulla (RVM), an integral relay of the central descending pain modulation system. Furthermore, the chemogenetic activation of the LC-RVM circuit was found to significantly induce colorectal visceral hyperalgesia and anxiety-related psychiatric disorders in naïve mice. In a dextran sulfate sodium (DSS)-induced visceral pain model, the mice also presented colorectal visceral hypersensitivity and anxiety-related psychiatric disorders, which were associated with increased activity of the LC-RVM circuit; LC-RVM circuit inhibition markedly alleviated these symptoms. Furthermore, the chronic restraint stress (CRS) model precipitates anxiety-related psychiatric disorders and induces colorectal visceral hyperalgesia, which is referred to as pathological stress-induced hyperalgesia, and inhibiting the LC-RVM circuit attenuates the severity of colorectal visceral pain. Overall, the present study clearly demonstrated that the LC-RVM circuit could be critical for the comorbidity of colorectal visceral pain and stress-related psychiatric disorders. Both visceral inflammation and psychological stress can activate LC noradrenergic neurons, which promote the severity of colorectal visceral hyperalgesia through this LC-RVM circuit.

Keywords Pathological stress, Colorectal visceral pain, Locus coeruleus, Rostral ventromedial medulla, Neural circuit

Introduction

Pathological stress cannot be avoided in the present competitive world. Unlike physiological stress, which carries survival value, pathological stress is associated with detrimental effects on physical health and the occurrence of disease [21]. Pathological stress is often comorbid with alterations in gastrointestinal tract function, which in turn lead to visceral hyperalgesia [6, 30, 43, 49, 68]. Psychological and pharmacological interventions that mediate stress perception have been demonstrated to ameliorate visceral pain symptoms [57, 62]. In addition, visceral pain and stress-related psychiatric disorders

†Dexu Kong, Yunchun Zhang and Po Gao have contributed equally to this work

*Correspondence:
Yingfu Jiao
yingfujiao@yeah.net
Weifeng Yu
ywf808@yeah.net
Daxiang Wen
wdxrwj@126.com
[1] Department of Anesthesiology, Renji Hospital, Shanghai Jiaotong University School of Medicine, Shanghai 200127, China
[2] Key Laboratory of Anesthesiology (Shanghai Jiao Tong University), Ministry of Education, Shanghai, China

exhibit high comorbidity [12, 77], which tends to create a positive link between stress-related psychiatric disorders and visceral pain that is difficult to decouple when encountered in many acute and chronic clinical settings [76]. The mechanisms of this association warrant more research attention.

As the major producer of noradrenaline (NA) in the central nervous system, the locus coeruleus (LC) sends widespread projections throughout the central nervous system and acts as the main stress-responsive nucleus implicated in mediating psychiatric disorders [45, 63, 69]. Because the chemogenetic blockade of the LC-basolateral amygdala circuit can reverse pain-induced psychiatric disorders but has no effect on the emergence of sensory hyperalgesia [41], the LC may contribute to pain and stress-related psychiatric disorders through distinct neural circuits. In addition, previous findings suggested that stress elicits visceral hyperalgesia and the functional reorganization of pain circuits, including functional activation of the LC [1, 37, 38, 42, 52, 61]; however, responses to colorectal distention were inhibited during coeruleospinal (LC/SC) electrical stimulation [36, 37]. These results suggest that the LC may mediate stress-induced visceral hyperalgesia through other neural circuits rather than the classical descending LC/SC projection.

The rostral ventromedial medulla (RVM) is a key relay in the descending pain modulation system [13, 20]. Electrical or chemical stimulation of the RVM produces either descending inhibition or pain by regulating spinal dorsal neuron responses and spinal nociceptive reflexes to noxious stimuli [10, 48, 51, 65]. In terms of visceral pain, several studies have implicated a major role for the RVM in central processing of visceral pain, such as urinary bladder distention [54], pancreatic pain [73], colorectal distention and visceral hyperalgesia induced by chemical intracolonic irritants [35, 78]. Furthermore, previous studies have observed functional connectivity between the RVM and LC by using resting-state functional magnetic resonance imaging and fiber photometry systems. Specifically, changes in neuronal responses in the RVM and LC to stress stimuli or visceral nociceptive stimuli were identified [28, 29, 47, 50]. Overall, these findings suggest that the LC-RVM circuit may be a convergence point between stress and colorectal visceral pain, but the detailed neural circuit and cause-and-effect relationship between the LC and RVM in stress-induced visceral pain remain far from clear.

In this study, we used retrograde labeling and projection-specific chemogenetic manipulation of the LC-RVM circuit in mice to determine the precise role of the LC-RVM circuit in stress-induced effects on visceral pain. To this end, a model of the comorbidity of stress and colorectal visceral pain induced by dextran sulfate sodium (DSS) and chronic restraint stress (CRS) was used.

Materials and methods

Animals

Naïve male C57BL/c mice obtained from the vivarium of Shanghai Jiaotong University School of Medicine were used in all experiments. Animals weighed 22–26 g (6–8 weeks of age) and were housed in a temperature-controlled room (22–25 °C) illuminated from 07:00 to 19:00. Food and water were available ad libitum. All animal care and experimental procedures followed the Guiding Principles on the Care and Use of Animals and the Animal Management Rule of the Ministry of Public Health, People's Republic of China (documentation 545, 2001) and were approved by the Ethnic Committee for Experimental Use of Animals of Shanghai Jiaotong University School of Medicine.

Stereotaxic injection

Cre-dependent adeno-associated viruses (AAVs) were used to manipulate neural activity in the LC in this study. AAV injections and cranial window implantations were performed as previously described [15, 59]. Mice were deeply anesthetized with pentobarbital sodium by intraperitoneal injection (i.p.) (0.1 g/kg) and positioned in a stereotaxic apparatus (RWD, Shenzhen, China). The skull was exposed via a small incision, and three small holes were drilled (0.50 mm drill bit) into the skull to introduce a microinjection glass pipette into bilateral LC (AP, −5.40 mm, ML, ± 0.80 mm, DV, 3.80 mm) in a volume of 150 nL for each side at 15 nL/min and into the RVM (AP, −5.70 mm, ML, 0.00 mm, DV, 5.80 mm) in a volume of 300 nL at 30 nL/min. The syringe was slowly retracted after an additional 10 min diffusion of the virus. The skin was sutured, and the animals were allowed to recover in prewarmed cages before returning to the home cage. Postoperative antibiotic therapy was administered in the form of ceftriaxone sodium 3 days after surgery (i.p.) (0.1 g/kg/day, once a day).

For LC→RVM circuit tracing, a dual viral approach was performed to label the LC neurons projecting to the RVM: bilateral injection of AAV2/9-CAG-DIO-mCherry-WPRE ($\sim 1.1 \times 10^{12}$ vg/mL) targeting the LC and of AAV2/retro-CMV-Cre-WPRE ($\sim 2.00 \times 10^{12}$ vg/mL) targeting the RVM. To selectively label the NA^{LC}→RVM circuit, AAV2/9-CAG-DIO-EGFP-WPRE ($\sim 2.0 \times 10^{12}$ vg/mL) was bilaterally injected into the LC and AAV2/retro-TH-Cre ($\sim 2.00 \times 10^{12}$ vg/mL) into the RVM.

For chemogenetic manipulation, AAV2/9-CAG-DIO-hM3D(Gq)-mCherry (hM3Dq-mCh) ($\sim 2.00 \times 10^{12}$ vg/mL) or AAV2/9-CAG-DIO-hM4D(Gi)-mCherry (hM4Di-mCh) ($\sim 2.00 \times 10^{12}$ vg/mL) was bilaterally injected into the LC, and AAV2/9-CAG-DIO-mCherry (mCh) ($\sim 2.00 \times 10^{12}$ vg/mL) was used as the control together with AAV2/retro-TH-Cre ($\sim 2.00 \times 10^{12}$ vg/mL) injection into the RVM. Mice were used 3 weeks after AAV injection. All viruses were purchased from Brain-VTA (Wuhan, China).

Chemogenetic manipulation

For the chemogenetic manipulation of the $NA^{LC} \rightarrow RVM$ circuit, mice were injected (i.p.) (0.03 mg/kg dissolved in normal saline) for activation or (i.p.) (0.1 mg/kg dissolved in normal saline) for inhibition with clozapine 30 min before behavioral assessment, unless otherwise stated. Controls received an equivalent volume of saline. This dosage of clozapine was selected based on published studies [22].

Dextran sulfate sodium administration

To induce DSS colitis, mice were offered filter-sterilized 2.5% (w/v) DSS (Mpbio, Canada) as their sole drinking water for 7 days ad libitum [18]. Mice were monitored, and the disease activity index score was determined as described previously, including assessments of diarrhea, rectal bleeding, and initial weight loss. Scores were defined as follows: diarrhea score 0 (normal), 2 (soft), or 4 (watery stool), and rectal bleeding score 0 (no blood), 2 (visual pellet bleeding), or 4 (gross bleeding, blood around anus) [33]. Weight loss was measured as a percentage relative to the initial weight of each individual. The distal colons were dissected after DSS treatment (Day 7) and compared with those of the control group rats that received only normal drinking water throughout the experimental period.

Restraint stress

The restraint stress model was used to study psychological stress [16]. Restraint stress was performed as described previously [60]. Briefly, mice in the chronic restraint stress (CRS) group were immobilized for 2 hours daily for 14 consecutive days in 50 mL conical tubes with holes to allow the mice to breath. Mice in the acute restraint stress (ARS) group were immobilized once for 2 h. The control group (Con) was allowed to freely move in the cage without access to water or food. In addition, the CRS combined with 1% DSS model was used to replicate the common condition that psychological stress predispose the individual to develop visceral hyperalgesia.

Abdominal mechanical sensitivity

The abdominal mechanical sensitivity of mice was measured using abdominal withdrawal reflex (AWR) tests as described previously [3, 35]. Briefly, mice were habituated to a metallic mesh floor covered with plastic boxes for 1 h daily for 3 days prior to testing, and the abdomen was shaved 1 day before experiments. The abdominal area was stimulated with calibrated von Frey filaments (VFFs) of different applied forces (subthreshold mechanical stimuli ("allodynia" corresponds to 0.07 g force application) and painful stimuli ("hyperalgesia" thicker filaments, correspond to 0.16 and 1 g force application)) 10 times each for 5–8 s with 10 s intervals. Notably, the same point could not be stimulated twice in succession to avoid learning or sensitization. Data was expressed as the number of withdrawal responses of 10 applications, for which 0 indicated no withdrawal and 10 indicated the maximum number of withdrawals. Withdrawal responses were defined as (1) abdominal withdrawal from the VFFs, (2) consequent licking of the abdominal area, or (3) withdrawal of the entire body. All tests were performed in a blinded manner.

Open field test (OFT)

The open field test (OFT) was performed to assess stress-induced anxiety-related psychiatric disorders [7]. The apparatus consisted of an open-square grey arena (40×40 cm), 40 cm high, with the floor divided into 16 squares by black lines. Each mouse was placed at the center of the open-field box, and its horizontal movements were monitored for 30 min with a video camera. Decreased time and distance in the central area were indicative of the psychiatric disorders-related behaviors. The apparatus was thoroughly cleaned between each test.

Immunofluorescent staining

The $NA^{LC} \rightarrow RVM$ circuit was evaluated using immunofluorescent staining. The expression of c-Fos was examined to assess neuronal activity changes in the $NA^{LC} \rightarrow RVM$ circuit after in vivo chemogenetic manipulation or DSS administration in hM3Dq-, hM4Di- and control mCherry-injected mice, with clozapine i.p. injection treatment for 2 h before perfusion [8, 31]. Mice were transcardially perfused with phosphate buffered saline (PBS) followed by 4% paraformaldehyde. The brain tissues were then harvested, fixed overnight in 4% paraformaldehyde at 4 °C, cryoprotected in 30% sucrose at 4 °C until isotonic and embedded in OCT. Free-floating immunohistochemistry was performed with 20-μm-thick serial coronal brain sections. After washing and blocking in blocking solution, the sections were

incubated with primary antibodies, including both anti-c-Fos (1:500, rabbit, CST) and anti-TH (1:500, chk, Abcam) at 4 °C overnight, and with secondary antibodies (1:500, anti-rabbit Alexa Fluor 488, abcam and 1:500, anti-chk Alexa Fluor 405, abcam) at room temperature for 2 h. All antibodies were diluted in PBS prior to use. Confocal images were captured on an Olympus FV-1200 microscope.

Histopathologic examination

After evaluating macroscopic damage, segments of the distal colon were stapled flat, mucosal side up, onto cardboard and fixed in 10% neutral-buffered formalin for 24 h at 4 °C. Samples were then dehydrated in sucrose, embedded in paraffin, sectioned at 5 μm and mounted onto slides. Paraffin blocks were prepared and sectioned at a thickness of 5 μm. Subsequently, the sections were transferred into hematoxylin and eosin and examined. Finally, photographs were taken with a digital imaging system consisting of a digital camera and image analysis software (Image J).

The microscopic assessments consisted of 3 items (severity of inflammation, mucosal damage, and crypt damage), and the highest score used for analysis. The score of each variable was added to give a total microscopic damage score (maximum of 11). Scores were defined as follows: goblet cell depletion score 1 (normal) or 0 (absence); crypt damage score 1 (normal) or 0 (absence); destruction of mucosal architecture score 1 (normal), 2 (moderate) or 3 (extensive); extent of muscle thickening score 1 (normal), 2 (moderate) or 3 (extensive); and presence and degree of cellular infiltration score 1 (normal), 2 (moderate) or 3 (transmural). The microscopic total damage score was determined in a blinded fashion. The resected sections of distal colon from the normal mice showed intact epithelium, normal muscle architecture and absence of edema, which are microscopic signs of colonic damage. Loss of mucosal architecture, thickening of smooth muscle, presence of crypt abscesses and extensive cellular infiltration were observed in the DSS-treated mice colon specimens.

Statistical analysis

Statistical analyses were performed using GraphPad Prism 8 (GraphPad Software, San Diego, CA). Mice were randomly assigned to groups in all experiments. No animals or data points were excluded during analysis. The significance of the difference between two independent groups was determined using Student's t tests. For multigroup comparisons, we applied analysis of variance (one-way or two-way ANOVA). The results were considered significantly different at $P < 0.05$. Data are presented as the mean ± SEM. Statistical details for specific experiments are summarized in the figure legends.

Results

The characteristics of the NA^{LC}→RVM circuit and facilitation of psychiatric disorders and visceral hyperalgesia after chemogenetic activation of the NA^{LC}→RVM circuit

To elucidate the precise location of LC neurons projecting to the RVM that could be involved in the development of visceral pain, we first investigated the distribution of mCherry signals in coronal sections of the entire LC after utilizing the adenovirus tracer for neuronal connectivity (Fig. 1A). Notably, many mCherry signals were observed in the dorsal caudal LC segment, which differed from the location of neurons in the LC that projected to the spinal cord. These data suggested that dorsal caudal LC neurons send afferents to the RVM.

We next identified the cell types of LC neurons projecting to the RVM. As the LC is the main source of noradrenaline in the central nervous system [55], we used immunohistochemical staining against tyrosine hydroxylase (TH) to localize LC-noradrenergic neurons (NA^{LC}) (Fig. 1B) and marked the location of NA^{LC} projecting to the RVM (NA^{LC}→RVM) in each mouse (Fig. 1C). Approximately 96% of mCherry+ neurons in the LC were noradrenergic neurons.

To examine the role of the NA^{LC}→RVM circuit in psychiatric disorders and visceral hyperalgesia, we examined the effects of hM3D(Gq)-DREADD–mediated activation of this circuit in naïve mice (Fig. 2A). Neurons expressing the hM3Dq receptor can be activated by systemic clozapine administration (0.03 mg/kg i.p.). Immunostaining of c-Fos was carried out to evaluate the excitatory effect. As the results show, the expression of c-Fos remarkably increased after the administration of clozapine in the hM3Dq-mCh group compared with the mCh group. A total of 92.18% of the NA^{LC} projecting to the RVM were robustly activated (colocalized with c-Fos) compared with 11.99% in the mCh group (Fig. 2B).

Psychiatric disorders-related behaviors were evaluated by OFT immediately after clozapine injection, and the behavior of each mouse was recorded for 30 min. 5 min after administration of clozapine, hM3Dq-mCh mice displayed strongly suppressed locomotor activity and decreased distance moved. And they spent less time in the center of the open field (Fig. 2C, D).

Visceral pain-like hyperalgesia was assessed. Significant differences were found between the hM3Dq-mCh and the mCh groups. Clozapine increased abdominal responses in the hM3Dq-mCh group compared with the mCh group. By contrast, responses in the mCh group were not significantly different from the baseline (Fig. 2E). Thus, the activation of the NA^{LC}→RVM circuit could lead to anxiety-related psychiatric disorders and visceral hyperalgesia.

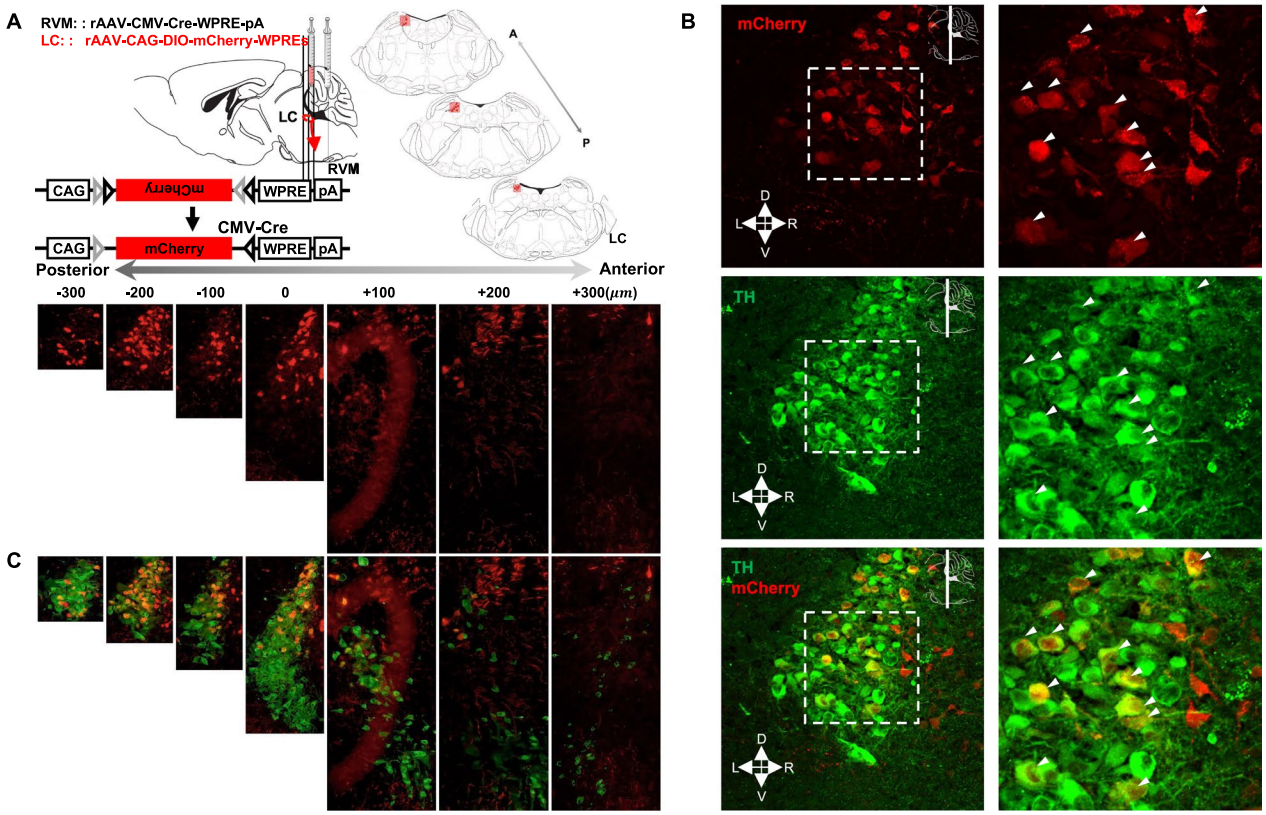

Fig. 1 Dissection of the locus coeruleus noradrenergic neurons→rostral ventromedial medulla (NA^{LC}→RVM) circuit. **A** Schematic diagram of injection and coronal sections of the LC. **B** Coronal section (at − 200 μm location) is shown. M: medial, D: dorsal, L: lateral, V: ventral. **C** mCherry (mCh) co-localizes with tyrosine hydroxylase (TH) in the LC derived from (**A**) and (**B**). Scale bars, 20 μm (**B**, Left), 50 μm (**B**, Right), 100 μm (**A**, Bottom and **C**)

Increased NA^{LC}→RVM circuit excitability in DSS-treated mice

We used the DSS-induced colorectal visceral pain model to identify whether the NA^{LC}→RVM circuit is generally involved in pathological pain. Successful induction of the model was confirmed by increased stool consistency, appearance of blood in the stool, a marked reduction in body weight (Fig. 3A) and increased microscopic damage scoring of colon samples (Fig. 3B) 7 days after DSS administration compared with the control group.

The psychiatric disorders of mice were assessed after DSS treatment. In the OFT (Fig. 3C), DSS-treated mice showed significant decreases in center crossing and center duration compared with those in the control group. In addition, the impaired mobility among the DSS-treated mice could reflect visceral pain.

(See figure on next page.)

Fig. 2 NA^{LC}→RVM circuit activation drives anxiety-related psychiatric disorders and colorectal visceral hyperalgesia. **A** Schematic diagram of injection and timeline of experimental procedure. **B** (Left) Representative images of c-Fos expression in TH+/mCh+ neurons in the LC in hM3Dq-mCh and Control mice. (Right) The percentage of TH+/mCh+/c-Fos+ neurons in TH+/mCh+ or c-Fos+ neurons in hM3Dq-mCh and mCh mice 2 h after clozapine i.p. ($n = 6$ slices from three mice; c-Fos+mCh/mCh, $t = 25.86$, $P < 0.0001$; c-Fos+mCh/c-Fos, $t = 1.406$, $P = 0.1899$, unpaired t test). **C-D** Line charts and bars show the distance moved and the time spent in the center as well as the total distance moved immediately after clozapine i.p. in hM3Dq-mCh and mCh mice ($n = 6$ per group; distance in center: main effect: $F_{(1, 110)} = 91.72$, $P < 0.0001$, interaction: $F_{(9, 110)} = 1.674$, $P = 0.1036$; time in center: main effect: $F_{(1, 110)} = 75.13$, $P < 0.0001$, interaction: $F_{(9, 110)} = 0.6825$, $P = 0.7233$, two-way ANOVA with Sidak post hoc tests; total distance: $t = 5.903$, $P = 0.0002$, unpaired t test). **E** Mechanical sensitivity of the abdomen was measured with calibrated (0.07, 0.16, and 1 g) von Frey filaments (VFFs) before and 2 h and 24 h after clozapine i.p. in hM3Dq-mCh and mCh mice ($n = 7$–8 per group; 0.07 g, main effect: $F_{(1, 39)} = 10.01$, $P = 0.0030$, interaction: $F_{(2, 39)} = 9.765$, $P < 0.0004$; 0.16 g, main effect: $F_{(1, 39)} = 8.472$, $P = 0.0059$, interaction: $F_{(2, 39)} = 4.873$, $P = 0.0129$; 1.0 g, main effect: $F_{(1, 39)} = 5.634$, $P = 0.0226$, interaction: $F_{(2, 39)} = 6.952$, $P = 0.0026$, two-way ANOVA with Sidak post hoc tests). Scale bars, 20 μm (**B**, Right), 50 μm (**B**, Left). Data represent mean ± SEM. *$P < 0.05$, **$P < 0.01$, ***$P < 0.001$, ****$P < 0.0001$

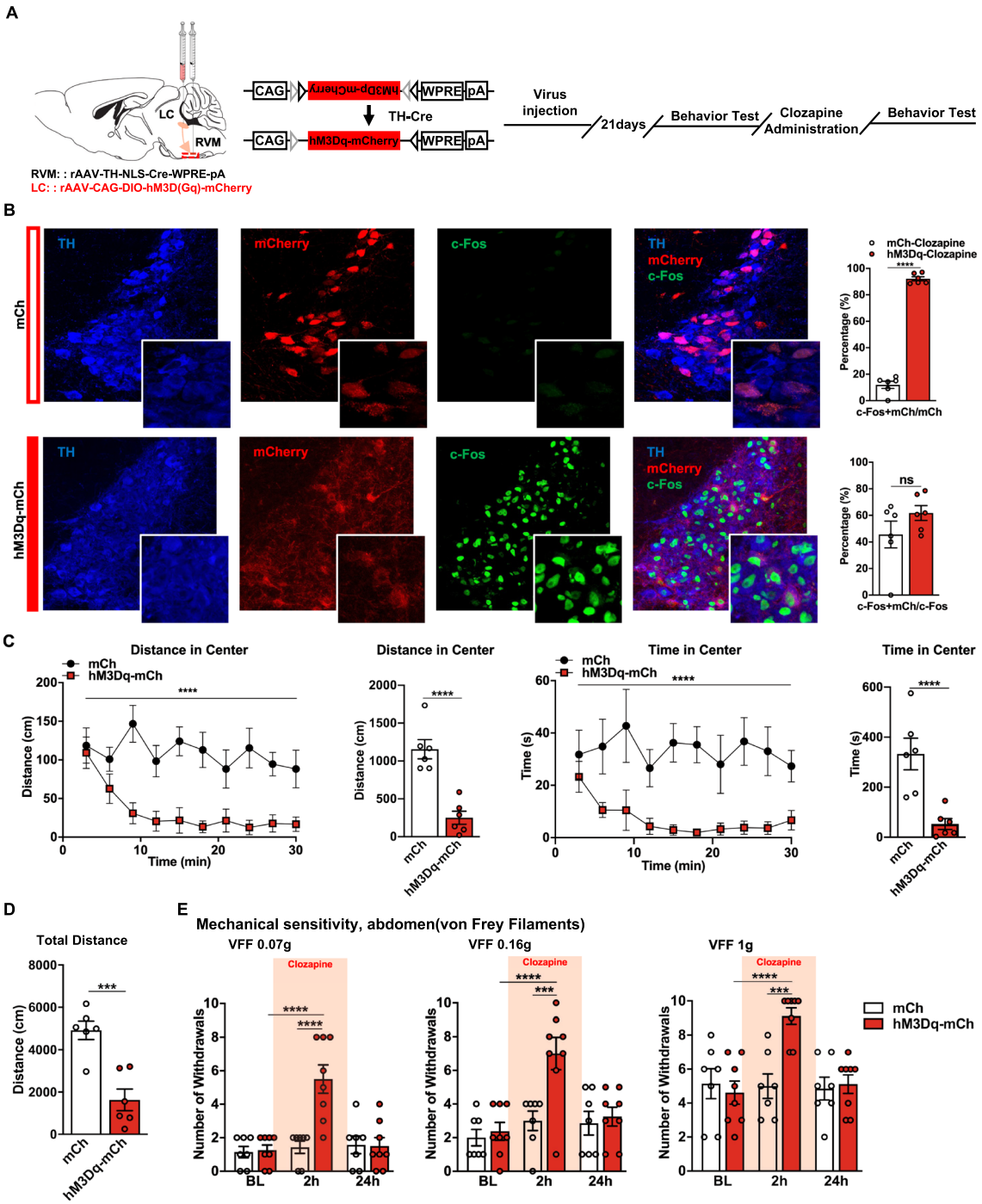

Fig. 2 (See legend on previous page.)

Furthermore, the mean response frequencies of DSS-treated mice were significantly elevated compared to those of water-only treated mice at 7 days in the abdominal mechanical sensitivity evaluation (Fig. 3D). These results suggested that DSS administration successfully induced anxiety-related psychiatric disorders and colorectal visceral hyperalgesia.

To assess the neuronal excitability of the NA^{LC}→RVM circuit in visceral pain, we targeted noradrenergic neurons expressing TH by local injection of AAV2/9-CAG-DIO-EGFP into the LC after intra-RVM injection

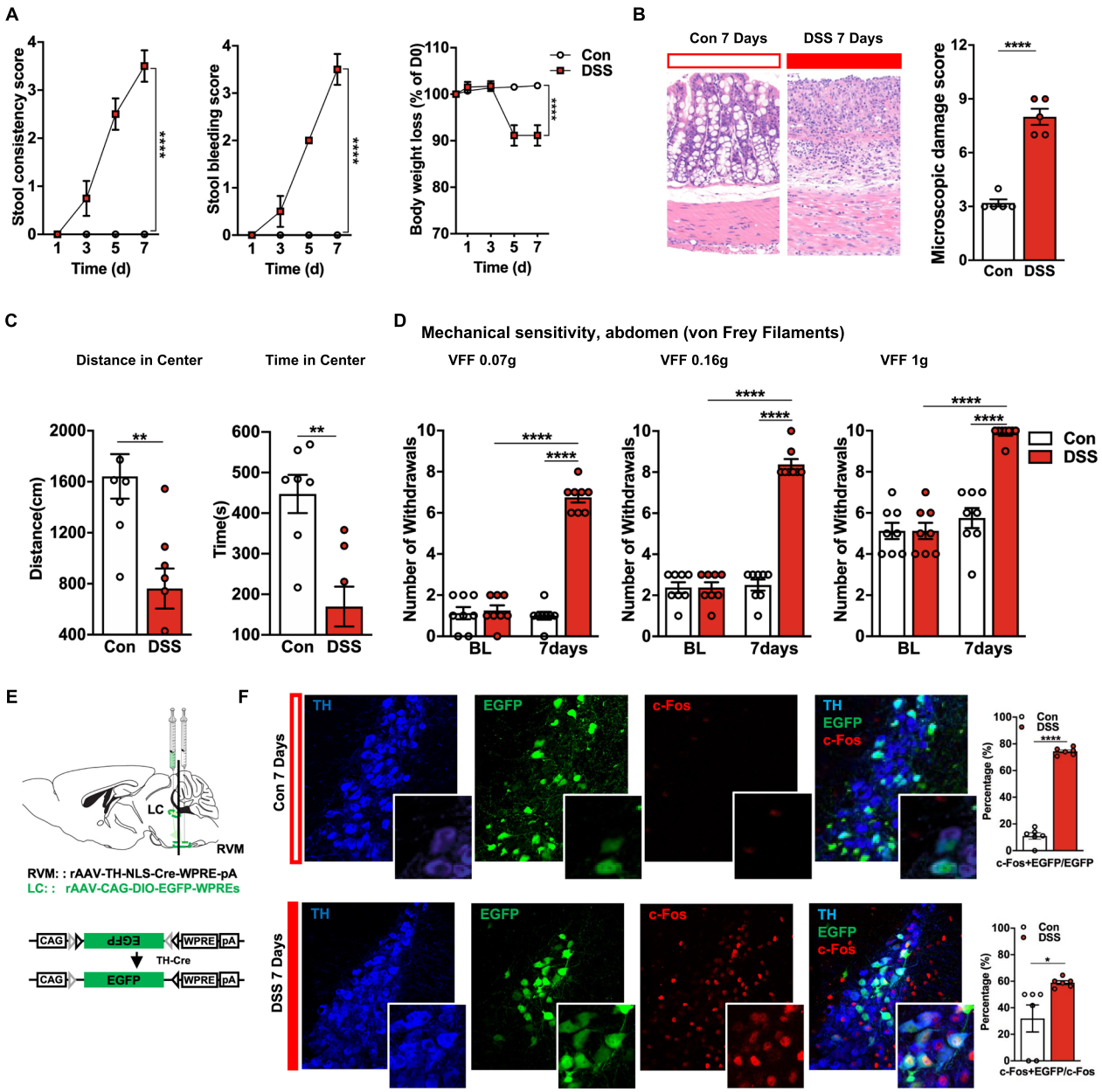

Fig. 3 Increased activity of the NA^{LC}→RVM circuit in DSS-treated mice. **A** The stool consistency score ($n = 8$ per group, interaction: $F_{(3, 56)} = 29.38$, $P < 0.0001$), the stool bleeding score ($n = 8$ per group, interaction: $F_{(3, 56)} = 46.67$, $P < 0.0001$) and the body weight loss ($n = 8$ per group, interaction: $F_{(4, 70)} = 29.38$, $P < 0.0001$) (two-way ANOVA with Sidak post hoc tests) were evaluated daily. **B** The microscopic damage score was a total score for 5 items (goblet cell depletion score; crypt damage score; destruction of mucosal architecture score; extent of muscle thickening score and presence and degree of cellular infiltration score) (maximum of 11) ($n = 5$ per group, $t = 9.798$, $P < 0.0001$, unpaired t test). **C** Bars show the distance moved and the time spent in the center ($n = 8$ per group; distance in center, $t = 3.750$, $P = 0.0022$; time in center, $t = 4.077$, $P = 0.0015$, unpaired t test). **D** Mechanical sensitivity of the abdomen was measured with calibrated (0.07, 0.16, and 1 g) VFFs in DSS and Control mice ($n = 8$ per group; 0.07 g, main effect: $F_{(1, 28)} = 139.3$, $P < 0.0001$, interaction: $F_{(1, 28)} = 127.7$, $P < 0.0001$; 0.16 g, main effect: $F_{(1, 28)} = 123.7$, $P < 0.0001$, interaction: $F_{(1, 28)} = 123.7$, $P < 0.0001$; 1.0 g, main effect: $F_{(1, 28)} = 29.66$, $P < 0.0001$, interaction: $F_{(1, 28)} = 29.66$, $P < 0.0001$, two-way ANOVA with Sidak post hoc tests). **E** Schematic diagram of injection. **F** (Left) Representative images of c-Fos expression in TH+/EGFP+ neurons in the LC in DSS and Control mice. (Right) The percentage of TH+/EGFP+/c-Fos+ in TH+/EGFP+ or c-Fos+ neurons in DSS and control mice ($n = 6$ slices from 3 mice for each group; c-Fos + EGFP/EGFP, $t = 23.66$, $P < 0.0001$; c-Fos + EGFP/c-Fos, $t = 2.624$, $P = 0.0254$, unpaired t test). Scale bars, 20 μm (**F**, Left), 50 μm (**F**, Right). Data represent mean ± SEM. $^{*}P < 0.05$, $^{**}P < 0.01$, $^{****}P < 0.0001$

of AAV2/retro-TH-Cre to selectively highlight the NA^{LC}→RVM circuit (Fig. 3E) and investigated the density of c-Fos-positive neurons coexpressing EGFP in the LC. We found that 74.36% of NA^{LC} projecting to the RVM were activated (colocalized with c-Fos) in the DSS group compared with 10.95% in the Con group (Fig. 3F). These results suggested an increase in neuronal excitability of the NA^{LC}→RVM circuit in DSS-induced colorectal visceral pain mice.

Chemogenetic inhibition of the NA^{LC}→RVM circuit attenuates DSS-induced psychiatric disorders and visceral hyperalgesia

Given the increased neuronal excitability of the NA^{LC}→RVM circuit in DSS-induced colorectal visceral pain mice, we subsequently aimed to investigate whether the inhibition of the neuronal excitability of the NA^{LC}→RVM circuit restored colorectal visceral hyperalgesia and anxiety-related psychiatric disorders in DSS-induced visceral pain mice (Fig. 4A). Neurons expressing hM4D(Gi) could be inhibited by systemic clozapine administration (0.1 mg/kg intraperitoneally). Immunostaining of c-Fos expression after 2 h of clozapine administration showed a dramatic decrease in the density of c-Fos-positive neurons coexpressing hM4Di-mCh in the LC compared with the mCh group. Only 10.16% of NA^{LC} projecting to the RVM were activated (colocalized with c-Fos) compared with 74.47% in the Con group (Fig. 4B). Psychiatric disorders-related behaviors were evaluated with 30 min recordings immediately and at 2 and 4 h after clozapine administration in the hM4Di-mCh-DSS group. The results showed that inhibiting NA^{LC}→RVM circuit induced a significant increase in the distance moved and the time spent in the center of the open field for the DSS group (Fig. 4C). Subsequently, colorectal visceral hyperalgesia-related responses markedly decreased in the hM4Di-mCh-DSS group at 2 and 4 h after clozapine administration. Responses in the DSS-mCh group were not significantly different from baseline at all assessed time points (Fig. 4D). Interestingly, in naïve mice, the inhibition of the NA^{LC}→RVM circuit has no affection on basal conditions based on locomotor and stress-related behaviors and pain threshold tests (Fig. 5A-C). Together, these findings indicate a crucial role of the NA^{LC}→RVM circuit in maintaining anxiety-related psychiatric disorders and colorectal visceral hyperalgesia in the current visceral pain model, while this circuit should be quiescent in the physiological state.

Critical role of the NA^{LC}→RVM circuit in stress-induced colorectal visceral hyperalgesia

Based on the previous results, we subsequently investigated the specific involvement of the NA^{LC}→RVM circuit in stress-induced colorectal visceral hyperalgesia. The CRS model was used to induce anxiety-related psychiatric disorders and the CRS combined with 1% DSS model was used to replicate the common condition that psychiatric disorders predispose the individual to develop visceral hyperalgesia (Fig. 6A). In the OFT, the mice in both groups displayed significant anxiety-related psychiatric disorders compared with the control group (Fig. 6B). Interestingly, colorectal visceral hyperalgesia-related behavior was also observed in the CRS group, while it was absent in the control and ARS groups (Fig. 6C and D). These results suggested that the current CRS and CRS combined with 1% DSS treatment models reliably induced colorectal visceral hyperalgesia behavior. We next investigated whether the inhibition of the neuronal excitability of the NA^{LC}→RVM circuit restored stress-induced colorectal visceral hyperalgesia. The chemogenetic inhibition of the NA^{LC}→RVM circuit did decrease colorectal visceral hyperalgesia-related responses in the CRS and CRS combined with 1% DSS treatment mice (Fig. 6E and F). In addition, activation of the NA^{LC}→RVM circuit produces anxiety-related psychiatric disorders and colorectal visceral hyperalgesia, but acutely inhibiting colorectal visceral hyperalgesia with morphine (0.2% 0.1 ml/10 g i.p.) had no anti-psychiatric disorders effects. We found that the movement distance and time spent at the center of the open field

(See figure on next page.)

Fig. 4 Decreasing the neuronal excitability of the NA^{LC}→RVM circuit attenuates anxiety-related psychiatric disorders and colorectal visceral hyperalgesia. **A** Schematic diagram of injection and timeline of experimental procedure. **B** (Left) Representative images of c-Fos expression in TH+/mCh+ neurons in the LC in DSS and control mice. (Right) The percentage of TH+/mCh+/c-Fos+ neurons in TH+/mCh+ or c-Fos+ neurons in hM4Di-mCh- and mCh-DSS mice 2 h after clozapine i.p. ($n = 6$ slices from three mice; c-Fos + mCh/mCh, $t = 9.539$, $P < 0.0001$; c-Fos + mCh/c-Fos, $t = 6.609$, $P < 0.0001$, unpaired t test). **C** Line charts and bars show the distance moved and the time spent in the center immediately, 2 h and 4 h after clozapine i.p. in hM4Di-mCh-DSS mice ($n = 4$–6 per group; distance in center, main effect: $F_{(2, 110)} = 33.50$, $P < 0.0001$; time in center, main effect: $F_{(2, 110)} = 13.71$, $P < 0.0001$, two-way ANOVA with Sidak post hoc tests). **D** Mechanical sensitivity of the abdomen was measured with calibrated (0.07, 0.16, and 1 g) VFFs before and 30 min, 2 h, 4 h and 24 h after clozapine i.p. in DSS mice expressing hM4Di-mCh or mCh ($n = 13$ per group; 0.07 g, main effect: $F_{(1, 117)} = 146.1$, $P < 0.0001$, time: $F_{(4, 117)} = 21.08$, $P < 0.0001$, interaction: $F_{(4, 117)} = 20.32$, $P < 0.0001$; 0.16 g, main effect of group: $F_{(1, 117)} = 80.57$, $P < 0.0001$, time: $F_{(4, 117)} = 21.60$, $P < 0.0001$, interaction: $F_{(4, 117)} = 19.36$, $P < 0.0001$; 1.0 g, main effect of group: $F_{(1, 117)} = 45.76$, $P < 0.0001$, time: $F_{(4, 117)} = 21.59$, $P < 0.0001$, interaction: $F_{(4, 117)} = 16.78$, $P < 0.0001$, two-way ANOVA with Sidak post hoc tests). Scale bars, 20 μm (**B**, Right) and 50 μm (**B**, Left). Data represent mean ± SEM. *$P < 0.05$, **$P < 0.01$, ***$P < 0.001$, ****$P < 0.0001$

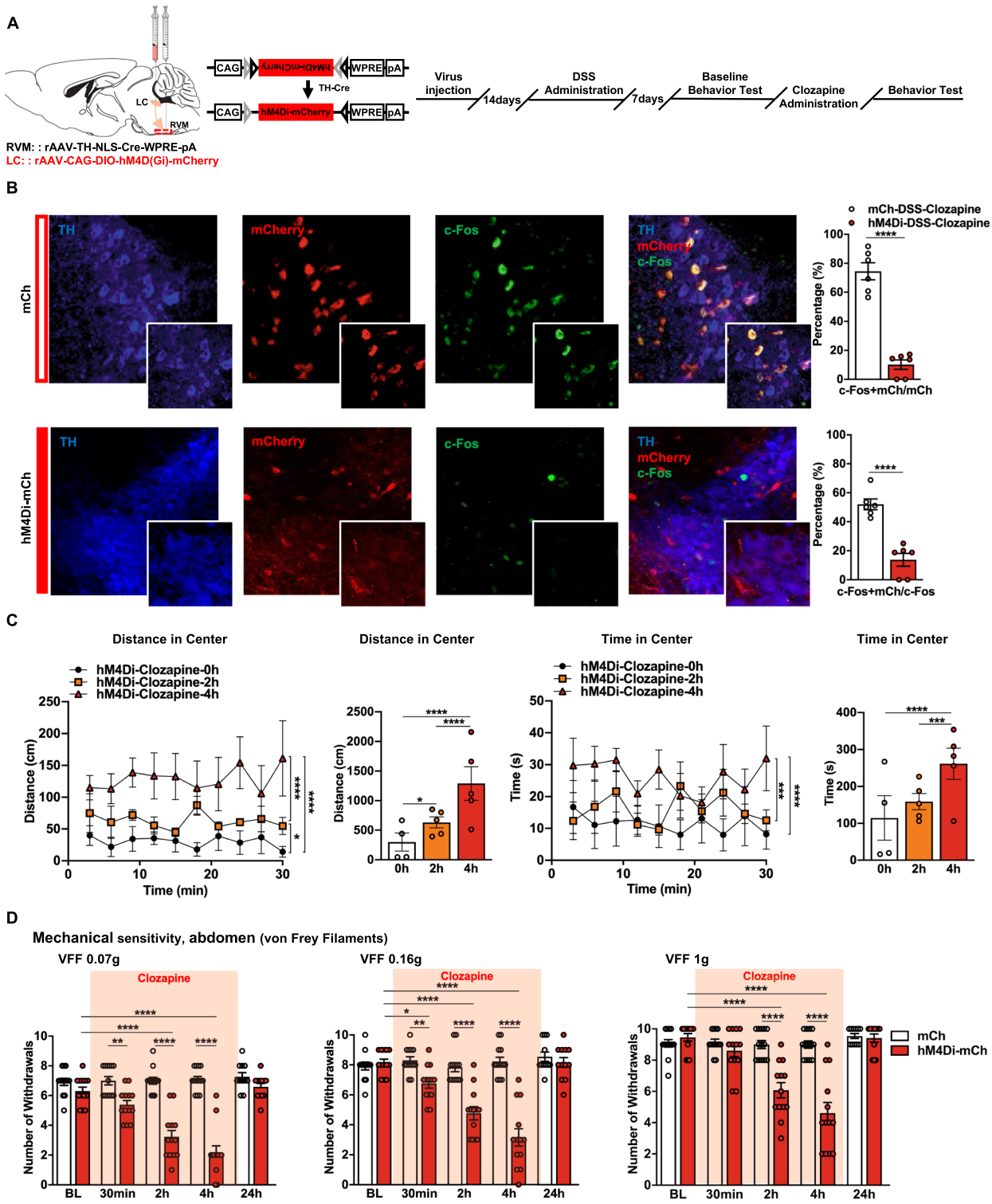

Fig. 4 (See legend on previous page.)

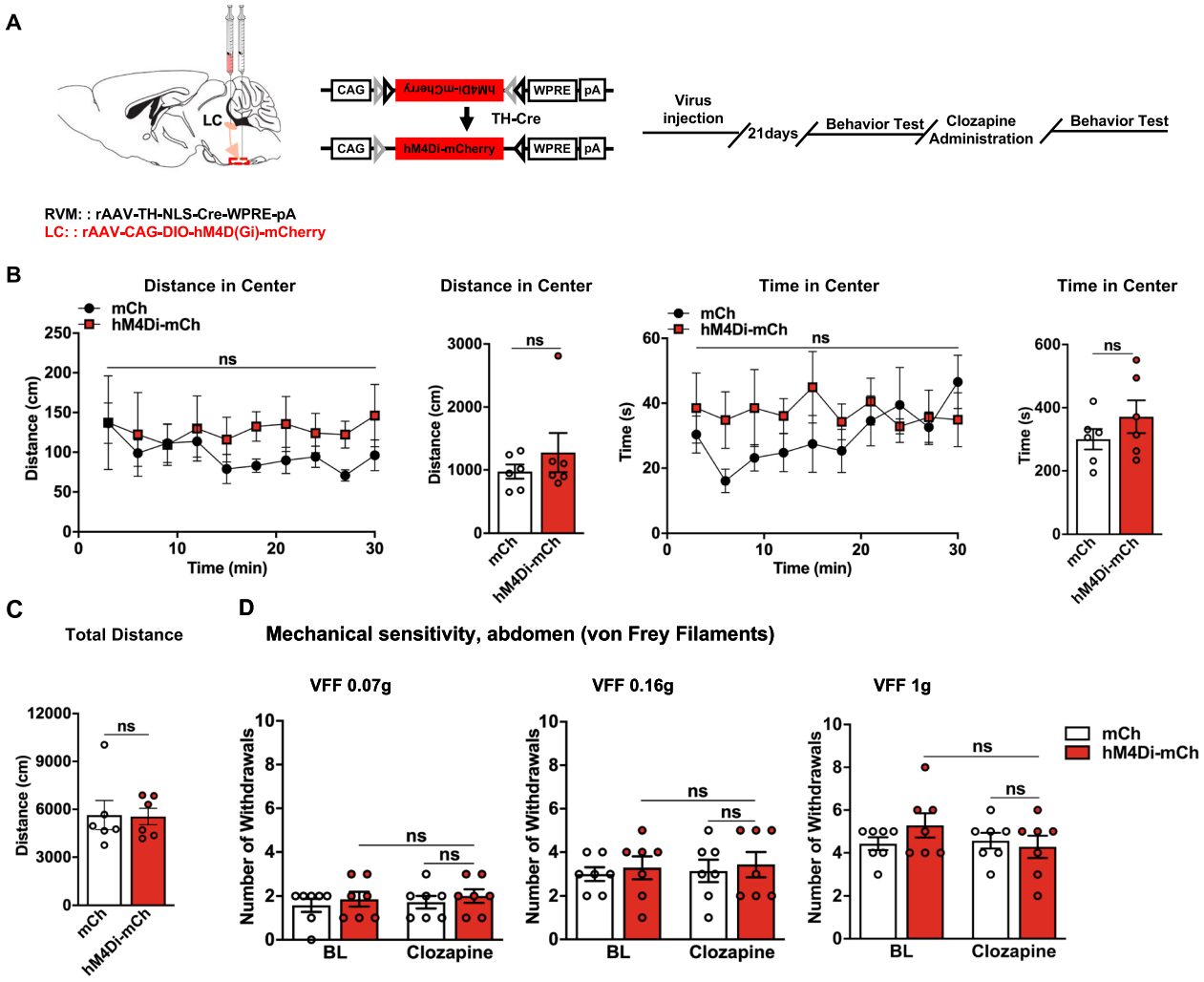

Fig. 5 Decreasing the neuronal excitability of the NA^{LC}→RVM circuit has no effect on basal conditions. **A** Schematic diagram of injection and timeline of experimental procedure. **B** Bars show the distance moved and the time spent in the center as well as the total distance immediately after administration of clozapine ($n = 6$ per group; distance in center: main effect: $F_{(1, 100)} = 5.488$, $P = 0.0211$, interaction: $F_{(9, 100)} = 0.2461$, $P = 0.9865$; time in center: main effect: $F_{(1, 100)} = 4.131$, $P = 0.0448$, interaction: $F_{(9, 100)} = 0.8160$, $P = 0.6027$, two-way ANOVA with Sidak post hoc tests). **C** Bars show the total distance moved after administration of clozapine i.p. in the hM4Di-mCh and mCh mice ($n = 6$ per group; total distance: $t = 0.08644$, $P = 0.9328$, unpaired t test). **D** Mechanical sensitivity of the abdomen was measured with calibrated (0.07, 0.16, and 1 g) VFFs before and 1 h after administration of clozapine in mice expressing hM4Di-mCh or mCh ($n = 7$ per group; 0.07 g, main effect: $F_{(1, 24)} = 0.8571$, $P = 0.3638$, interaction: $F_{(1, 24)} = 0.000$, $P > 0.9999$; 0.16 g, main effect: $F_{(1, 24)} = 0.3429$, $P = 0.5637$, interaction: $F_{(1, 24)} = 3.313e\text{-}030$, $P > 0.9999$; 1.0 g, main effect: $F_{(1, 24)} = 0.4000$, $P = 0.5331$, interaction: $F_{(1, 24)} = 1.600$, $P = 0.2180$ two-way ANOVA with Sidak post hoc tests). Data represent mean ± SEM. ns, no significance

were similar, but the total distance of locomotor activity increased in the hM3Dq-mCh-clozapine-morphine group compared with the hM3Dq-mCh-clozapine group (Fig. 7A–C). These results suggested a crucial role of the NA^{LC}→RVM circuit in the development of stress-induced colorectal visceral hyperalgesia instead of colorectal visceral pain-facilitated psychiatric disorders.

Discussion

Our study demonstrated a previously unappreciated NA^{LC}→RVM circuit that mediates stress-induced colorectal visceral hyperalgesia. Specifically, stress could activate LC noradrenergic neurons that project to the RVM and induced enhanced visceral pain sensation via the RVM-related descending pain facilitation pathway.

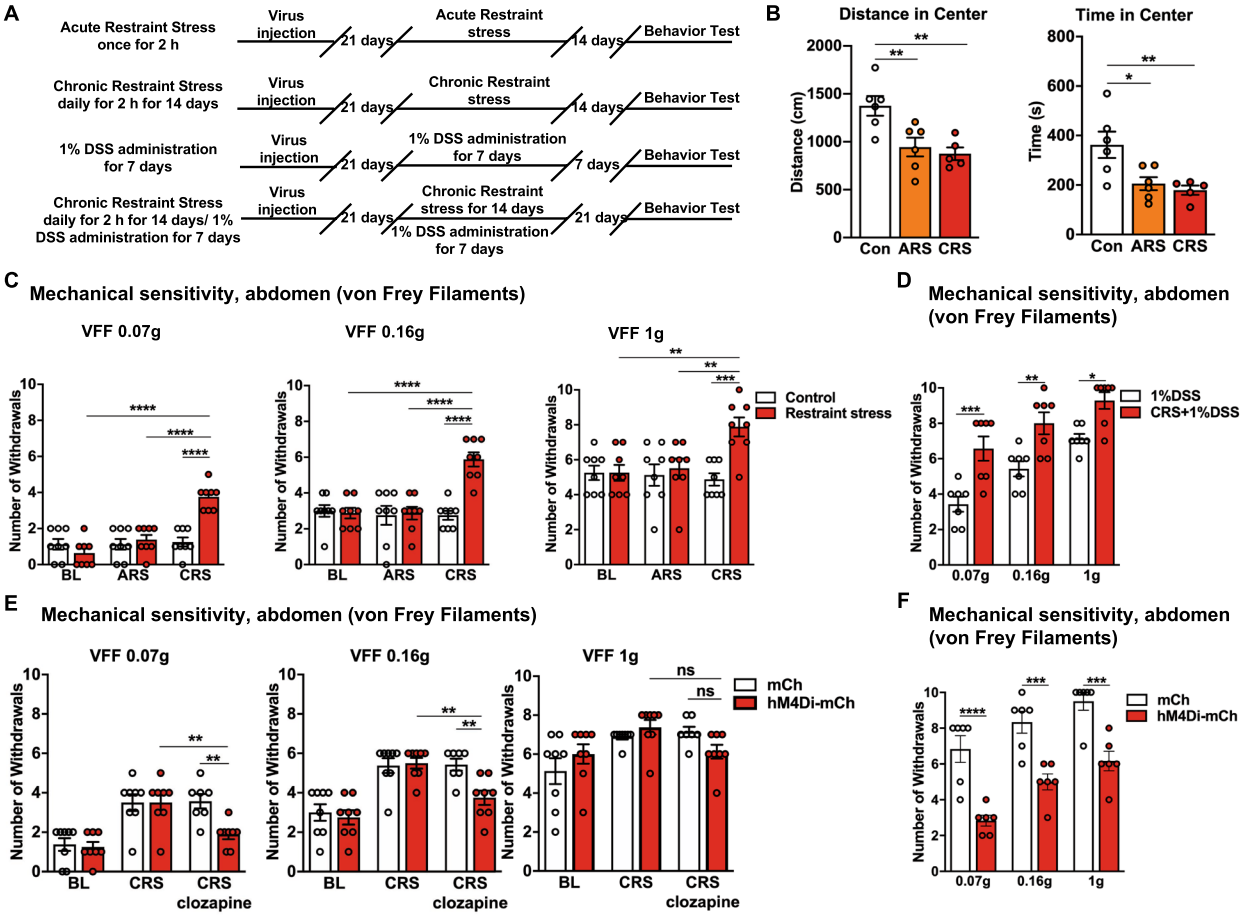

Fig. 6 Decreasing the neuronal excitability of the NA^{LC}→RVM circuit attenuates CRS-induced anxiety-related psychiatric disorders and colorectal visceral hyperalgesia. **A** Timeline of experimental procedure. **B** Bars show the distance moved and the time spent in the center in the ARS, CRS, and control mice ($n=6$ per group; distance in center,$F_{(2,14)}=8.401$, $P=0.0040$; time in center, $F_{(2,14)}=6.946$, $P=0.0080$, one-way ANOVA with Dunnett post hoc analysis). **C** Mechanical sensitivity of the abdomen was measured in the ARS, the CRS and the control mice ($n=8$ per group; 0.07 g, main effect: $F_{(1,42)}=11.57$, $P=0.0015$, interaction: $F_{(2,42)}=16.71$, $P<0.0001$; 0.16 g, main effect: $F_{(1,42)}=11.99$, $P=0.0012$, interaction: $F_{(2,42)}=12.04$, $P<0.0001$; 1.0 g, main effect of group: $F_{(1,42)}=7.628$, $P=0.0085$, interaction: $F_{(2,42)}=5.368$,$P=0.0084$, two-way ANOVA with Tukey post hoc tests). **D** Mechanical sensitivity of the abdomen was measured in the 1% DSS and CRS + 1% DSS mice ($n=7$ per group, main effect: $F_{(1,36)}=40.88$, $P<0.0001$, interaction: $F_{(2,36)}=0.50$, $P=0.6107$, two-way ANOVA with Sidak post hoc tests). **E** Mechanical sensitivity of the abdomen was measured before and 2 h after clozapine i.p. in control and hM4Di-mCh- or mCh-CRS mice ($n=7$–8 per group; 0.07 g, main effect: $F_{(1,41)}=4.666$, $P=0.0367$, interaction: $F_{(2,41)}=3.686$, $P<0.0337$; 0.16 g, main effect: $F_{(1,41)}=4.279$, $P=0.0449$, interaction: $F_{(2,41)}=3.500$, $P=0.0395$; VFFs 1.0 g, main effect: $F_{(1,41)}=0.1187$,$P=0.7322$, interaction: $F_{(2,41)}=2.746$, $P=0.0760$, two-way ANOVA with Tukey post hoc tests). **F** Mechanical sensitivity of the abdomen was measured before and 2 h after clozapine i.p. in hM4Di-mCh- or mCh-CRS + 1% DSS mice ($n=6$ per group, main effect: $F_{(1,30)}=64.00$, $P<0.0001$, interaction: $F_{(2,30)}=0.25$, $P=0.7804$, two-way ANOVA with Sidak post hoc tests). Data represent mean ± SEM. *$P<0.05$, **$P<0.01$, ***$P<0.001$, ****$P<0.0001$

Inhibiting this circuit effectively alleviates stress-induced colorectal visceral pain.

Accumulating evidences has demonstrated that LC neurons contribute to widespread projection networks throughout the central nervous system, and well-defined subpopulations of these neurons can encode distinct processes [52, 58, 70]. Therefore, the LC is assumed to be involved in both pain facilitation and alleviation [2, 19, 67]. Previously, visceral nociceptive responses of spinal dorsal horn neurons were reported to be inhibited by the descending LC-spinal circuit in the rat [27, 38]. Thus, the LC may exert a pro-nociceptive effect via a different circuit. Specifically, the activation of NA^{LC}→RVM projections found in this study facilitates colorectal visceral pain. The RVM has been recognized as a pain-gating nucleus responsible for integration of pain inhibition and facilitation processing since the early 1980s [56, 71, 72]. Although noradrenergic input to RVM nociceptive modulatory neurons has been reported [9, 46, 66] and interactions between the LC and RVM have been proven via

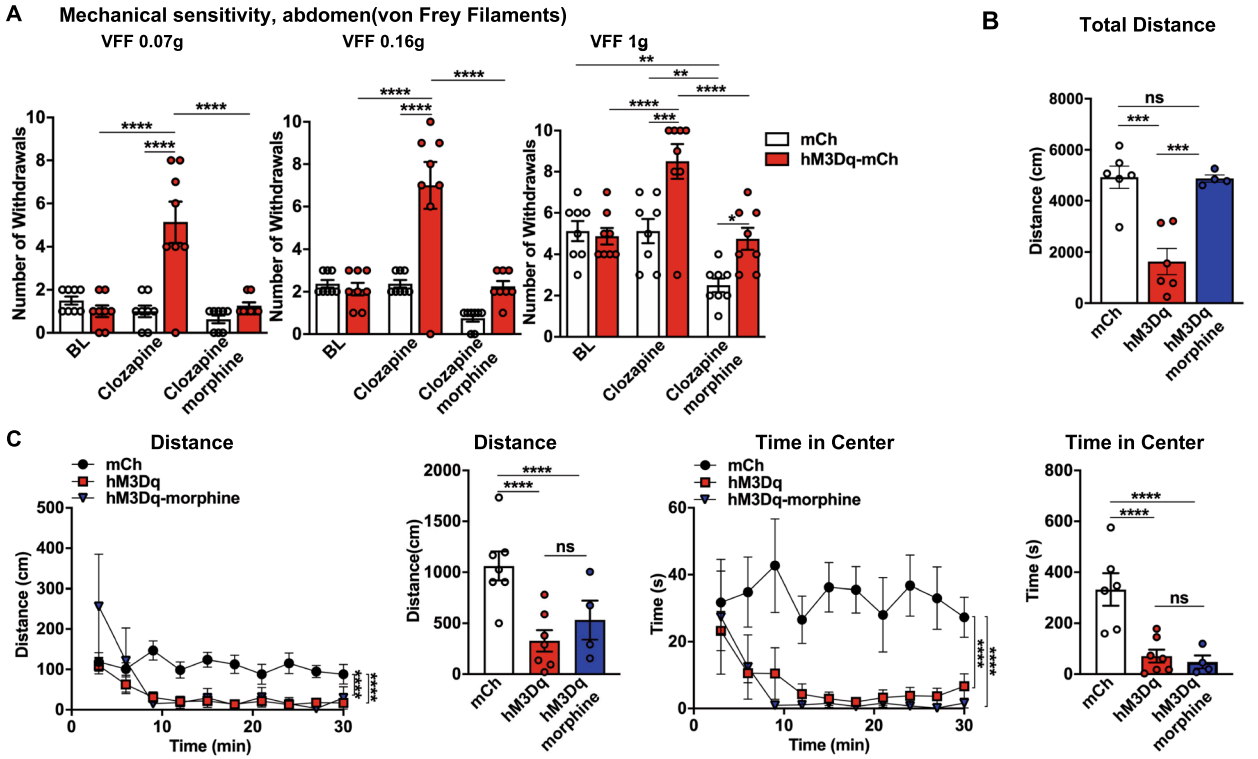

Fig. 7 The NA^{LC}→RVM circuit controls stress-induced colorectal visceral hyperalgesia. **A** Mechanical sensitivity of the abdomen was measured with calibrated (0.07, 0.16, and 1 g) VFFs before and 2 h after clozapine i.p. and 30 min after morphine i.p. which was followed by clozapine by 90 min i.p. in hM3Dq-mCh or mCh mice ($n = 8$ per group; 0.07 g, main effect: $F_{(1,42)} = 15.74$, $P = 0.0003$, interaction: $F_{(2,42)} = 15.21$, $P < 0.0001$; VFFs 0.16 g, main effect: $F_{(1,42)} = 23.68$,$P < 0.0001$, interaction: $F_{(2,42)} = 12.55$, $P < 0.0001$; VFFs 1.0 g, main effect: $F_{(1,42)} = 15.84$,$P = 0.0003$, interaction: $F_{(2,42)} = 5.663$, $P = 0.0066$, two-way ANOVA with Sidak post hoc tests). **B-C** Bars show the distance moved, the time spent in the center and the total distance moved immediately after clozapine i.p. followed after 30 min by morphine i.p. ($n = 6$ per group; total distance: $F_{(2,15)} = 8.416$, $P = 0.0035$, one-way ANOVA with Dunnett post hoc analysis; distance in center: main effect: $F_{(2,140)} = 25.44$,$P < 0.0001$, interaction: $F_{(18,140)} = 2.028$,$P = 0.0118$; time in center: main effect: $F_{(2,140)} = 53.61$, $P < 0.0001$, interaction: $F_{(18,140)} = 0.6189$, $P = 0.8802$, two-wayANOVAwith Tukey post hoc tests). Data represent mean ± SEM.*$P < 0.05$, **$P < 0.01$, ***$P < 0.001$, ****$P < 0.0001$

fMRI experiments, the precise role of this projection in pain modulation has never been studied. Our results suggest that LC-noradrenergic neurons send monosynaptic projections to the RVM and that the selective chemogenetic activation of LC neurons that project to the RVM elicits abdominal hyperalgesia in naïve mice. Considering these findings, we propose that the LC exerts an indirect pro-nociceptive effect of visceral pain due to its projections to the RVM. Indeed, unlike the visceral pain inhibition effect of known LC-spinal cord descending projections, the LC-RVM circuit in this study acts to promote visceral pain, which is consistent with the bidirectionally influence of the LC in pain modulation [24]. In addition, understanding the anatomical organization of the LC is critical to unlocking its function [52]. Counter to previous reports that showed that antinociceptive actions were evoked from a distinct, ventral subpopulation of LC neurons [24], we found that LC neurons projecting to the RVM were predominantly located in the dorsal part of the LC. This finding is aligned with the heterogeneity of LC and demonstrates the bidirectional regulation of nociception by LC [58].

Frequently, pathological stress tends to enhance visceral pain, coinciding with clinical observation [4, 17, 34], and the LC is a crucial component in both stress- and pain-related neural circuits [24, 32, 44, 69]. However, limited data elucidate the endogenous circuit mechanisms underlying stress and visceral pain interactions associated with the LC. The LC has only been thought to form part of a descending endogenous analgesic system that exerts inhibitory influences on spinal nociception [75]. The increased inhibition of the LC from the amygdala was once seen as a potential pain-enhancing mechanism for emotions processed in peripheral neuropathy [74]. Notably, this circuit does not participate in the promotion of emotion-induced visceral pain facilitation [74]. Theoretically, the heterogeneity of the LC and bidirectional modulation of nociception by the LC

leads to multifaceted effects on visceral pain through distinct neural circuits. In this study, DSS-induced colorectal visceral pain in mice lowered sensory thresholds and provoked a stress-related profile; meanwhile, the NA^{LC}→RVM circuit was significantly activated, as shown by significantly increased numbers of c-Fos-positive neurons in the LC. Interestingly, the chemogenetic activation of the NA^{LC}→RVM circuit in naïve mice instantly induced stress-related psychiatric disorders and subsequently, visceral hyperalgesia. In contrast, chemogenetic inhibition of the NA^{LC}→RVM circuit attenuates psychological maladaptation and pathological visceral hyperalgesia in the CRS and DSS models without affecting physiological pain sensation. Moreover, opioids are the frontline analgesics in pain management, and morphine is a potent opioid analgesic. The microinjection of morphine into the LC was shown to elicit analgesia through LC-Spinal cord projections, and it did not modify pain aversion [40]. Acute pain inhibition with morphine does not reverse the activity of the NA^{LC}→RVM circuit and does not attenuate psychiatric disorders-induced by the activation of this circuit. Therefore, these results seem to indicate that modulatin the NA^{LC}→RVM circuit affected both stress-related psychiatric disorders and pain sensory perception in the current animal models.

Earlier studies focused on the antinociceptive effects of RVM by exerting descending inhibitory effects on the spinal cord, but more recently, the RVM was shown to promote spinal pain signaling and increase nociceptive sensitivity. Multiple studies have also shown that RVM neurons play an important role in visceral hyperalgesia [54, 78], and noradrenergic inputs have been demonstrated to affect pain modulation by RVM neurons [5, 23]. In addition, we have demonstrated that activating the RVM receiving direct input from the NA^{LC} can enhance colorectal visceral pain perception in case of visceral inflammation-induced physical stress or restraint-induced psychological stress. Therefore, the LC can reasonably be assumed to be involved in stress-induced colorectal visceral pain via RVM. Noradrenaline plays a role in the modulation of pain in the RVM via α1- and α2-adrenoceptors on neurons. Previous studies have indicated that microinjecting α1 agonists and α2 agonists into the RVM increases and decreases nociceptive responses, respectively [26, 53]. Thus, the increased activation of α1-adrenoceptors from the LC on RVM neurons might cause an induced visceral pain-enhancing effect in mice with visceral inflammation or psychology-induced stress. However, the RVM has functionally distinct cell groups, and the cellular distribution and synaptic actions of α-receptor subtypes in the different cell groups are unknown. Thus, whether and how α receptors is involved in this circuit needs further investigation.

This study certainly has some important limitations. We did not address why chemogenetic manipulation of the NA^{LC}→RVM affects psychological maladaptation in this study, but we are very interested in this topic. The locus coeruleus (LC)-noradrenergic system is the main source of noradrenaline in the central nervous system and is intensively involved in modulating stress-related psychiatric disorders (major depressive disorder and anxiety) [45, 64]. When evaluating the chemogenetic activation of the LC, ongoing behaviors are rapidly interrupted and exploratory activity and anxiety are increased [25]. The chemogenetic blockade of LC neurons projecting to the ACC completely reverses depressive-like behavior [39]. Therefore, we cannot conclude that the NA^{LC}→RVM circuit is the only mechanism by which the LC modulates stress-psychiatric disorders, although the activation of this circuit is well known to instantly induce a robust suppression of locomotion and exploration. Indeed, we observed a strong increase in the number of c-Fos-positive NA^{LC} neurons, but this increase was not restricted to mCh coexpression in hM3Dq-mCh mice. The neuronal responses we observed may be mediated by local or distal polysynaptic recurrent circuits. In fact, our chemogenetic strategy specifically activates LC neurons and rapidly induces stress-related psychiatric disorders changes that last at least 30 min. Therefore, an increase in the activity of LC neurons projections to RVM activity might rapidly reconfigure large-scale brain networks to send projections to structure involved in emotions, which contribute to psychiatric disorders. Future investigations are needed to elucidate the involvement of this circuit in local or distal polysynaptic recurrent circuits. In addition, we mainly focused on visceral hyperalgesia, and a single OFT test was applied to assess psychiatric disorders. However, additional experiments (such as the plus-maze test and tail suspension test) could be helpful [11, 14] and will be included in a follow-up paper.

Overall, in addition to stress-related psychiatric disorders, our study extends LC function to colorectal visceral pain modulation through descending projections to the RVM, which are distinct from the LC/SC projections. The reorganization of the LC functional structure in the presence of stress will lead to activation of the NA^{LC}→RVM circuit to facilitate colorectal visceral pain, while the inhibition of this circuit can robustly alleviate stress-induced colorectal visceral pain. The LC likely acts as a relay center, exchanging information on stress-related psychiatric disorders and visceral pain. These findings provide a new perspective for exploring stress-induced pain sensation changes in neural circuits and raise the possibility of a novel therapeutic target for the management of stress-induced colorectal visceral hyperalgesia.

Abbreviations

AAVs	Adeno-associated viruses
ARS	Acute restraint stress
AWR	Abdominal withdrawal reflex
CRS	Chronic restraint stress
DREADD	Designer receptors exclusively activated by designer drugs
DSS	Dextran sulfate sodium
EGFP	An enhanced green fluorescent protein
hM3Dq	Human M3 muscarinic DREADD receptor coupled to Gq
hM4Di	Human M4 muscarinic DREADD receptor coupled to Gi
LC	Locus coeruleus
LC/SC	Coeruleospinal
mCh	mCherry fluorescent protein
NA	Noradrenaline
NA^{LC}	LC-noradrenergic neurons
$NA^{LC}\rightarrow$RVM	The NA^{LC} projecting to the RVM
OFT	Open field test
RVM	Rostral ventromedial medulla
TH	Tyrosine hydroxylase
VFFs	Von frey filaments

Acknowledgements
Not applicable.

Author contributions
DK, YZ, PG and YJ contributed to the experiment data acquisition, data analysis and the manuscript writing. CP and HD contributed to data acquisition. DK, YZ, SX, DT, JX, and PG contributed to critical resources and reagents. DK, YJ, WY and DW interpreted the results, designed the experiments and revised the paper. All authors edited and approved the manuscript.

Funding
This work was sponsored by the National Natural Science Foundation of China (Grants 81970478, 32030043, 82270916 and 32170995), the research project from Science and Technology Commission of Shanghai Municipality (19411951900), Shanghai Municipal Key Clinical Specialty (no. shslczdzk03601), the Key Specialty Construction Project of Pudong Health and Family Planning Commission of Shanghai (PWZXQ2017-06), the Innovative Research Team of High-level Local Universities in Shanghai (SHSMU-ZDCX20211102) and Shanghai Engineering Research Center of Peri-operative Organ Support and Function Preservation (20DZ2254200).

Availability of data and materials
All data generated or analysed during this study are included in this published article [and its supplementary information files].

Declarations

Ethics approval and consent to participate
Not applicable.

Consent for publication
Not applicable.

Competing interests
The authors have no conflicts of interest to declare.

Received: 11 December 2022 Accepted: 1 March 2023
Published online: 17 April 2023

References

1. Al-Adawi S, Dawe GS, Bonner A, Stephenson JD, Zarei M (2002) Central noradrenergic blockade prevents autotomy in rat: implication for pharmacological prevention of postdenervation pain syndrome. Brain Res Bull 57:581–586
2. Alba-Delgado C, Mico JA, Berrocoso E (2021) Neuropathic pain increases spontaneous and noxious-evoked activity of locus coeruleus neurons. Prog Neuropsychopharmacol Biol Psychiatry 105:110121
3. Barrot M (2012) Tests and models of nociception and pain in rodents. Neuroscience 211:39–50
4. Bennett EJ, Tennant CC, Piesse C, Badcock CA, Kellow JE (1998) Level of chronic life stress predicts clinical outcome in irritable bowel syndrome. Gut 43:256–261
5. Bie B, Fields HL, Williams JT, Pan ZZ (2003) Roles of alpha1- and alpha2-adrenoceptors in the nucleus raphe magnus in opioid analgesia and opioid abstinence-induced hyperalgesia. J Neurosci 23:7950–7957
6. Blanchard EB, Lackner JM, Jaccard J, Rowell D, Carosella AM, Powell C et al (2008) The role of stress in symptom exacerbation among IBS patients. J Psychosom Res 64:119–128
7. Bourin M, Petit-Demoulière B, Dhonnchadha BN, Hascöet M (2007) Animal models of anxiety in mice. Fundam Clin Pharmacol 21:567–574
8. Bravo L, Alba-Delgado C, Torres-Sanchez S, Mico JA, Neto FL, Berrocoso E (2013) Social stress exacerbates the aversion to painful experiences in rats exposed to chronic pain: the role of the locus coeruleus. Pain 154:2014–2023
9. Braz JM, Enquist LW, Basbaum AI (2009) Inputs to serotonergic neurons revealed by conditional viral transneuronal tracing. J Comp Neurol 514:145–160
10. Calejesan AA, Kim SJ, Zhuo M (2000) Descending facilitatory modulation of a behavioral nociceptive response by stimulation in the adult rat anterior cingulate cortex. Eur J Pain 4:83–96
11. Carola V, D'Olimpio F, Brunamonti E, Mangia F, Renzi P (2002) Evaluation of the elevated plus-maze and open-field tests for the assessment of anxiety-related behaviour in inbred mice. Behav Brain Res 134:49–57
12. Chen J, Winston JH, Fu Y, Guptarak J, Jensen KL, Shi X-Z, Green TA, Sarna SK (2015) Genesis of anxiety, depression, and ongoing abdominal discomfort in ulcerative colitis-like colon inflammation. Am J Physiol Regul Integr Comp Physiol 308:R18–R27
13. Chen Q, Heinricher MM (2019) Plasticity in the link between pain-transmitting and pain-modulating systems in acute and persistent inflammation. J Neurosci 39:2065–2079
14. Cryan JF, Mombereau C, Vassout A (2005) The tail suspension test as a model for assessing antidepressant activity: review of pharmacological and genetic studies in mice. Neurosci Biobehav Rev 29:571–625
15. Da Silva LFS, Walder RY, Davidson BL, Wilson SP, Sluka KA (2010) Changes in expression of NMDA-NR1 receptor subunits in the rostral ventromedial medulla modulate pain behaviors. Pain 151:155–161
16. Deng Y, Zhou M, Wang J, Yao J, Yu J, Liu W et al (2021) Involvement of the microbiota-gut-brain axis in chronic restraint stress: disturbances of the kynurenine metabolic pathway in both the gut and brain. Gut Microbes 13:1–16
17. Elsenbruch S, Rosenberger C, Enck P, Forsting M, Schedlowski M, Gizewski ER (2010) Affective disturbances modulate the neural processing of visceral pain stimuli in irritable bowel syndrome: an fMRI study. Gut 59:489–495
18. Esquerre N, Basso L, Defaye M, Vicentini FA, Cluny N, Bihan D et al (2020) Colitis-induced microbial perturbation promotes postinflammatory visceral hypersensitivity. Cell Mol Gastroenterol Hepatol 10:225–244
19. Farahani F, Azizi H, Janahmadi M, Seutin V, Semnanian S (2021) Formalin-induced inflammatory pain increases excitability in locus coeruleus neurons. Brain Res Bull 172:52–60
20. Fields HL, Bry J, Hentall I, Zorman G (1983) The activity of neurons in the rostral medulla of the rat during withdrawal from noxious heat. J Neurosci 3:2545–2552
21. Gao X, Cao Q, Cheng Y, Zhao D, Wang Z, Yang H et al (2018) Chronic stress promotes colitis by disturbing the gut microbiota and triggering immune system response. Proc Natl Acad Sci U S A 115:E2960–E2969
22. Gomez JL, Bonaventura J, Lesniak W, Mathews WB, Sysa-Shah P, Rodriguez LA et al (2017) Chemogenetics revealed: DREADD occupancy and activation via converted clozapine. Science 357:503–507
23. Haws CM, Heinricher MM, Fields HL (1990) Alpha-adrenergic receptor agonists, but not antagonists, alter the tail-flick latency when microinjected into the rostral ventromedial medulla of the lightly anesthetized rat. Brain Res 533:192–195

24. Hickey L, Li Y, Fyson SJ, Watson TC, Perrins R, Hewinson J et al (2014) Optoactivation of locus ceruleus neurons evokes bidirectional changes in thermal nociception in rats. J Neurosci 34:4148–4160
25. Hirschberg S, Li Y, Randall A, Kremer EJ, Pickering AE (2017) Functional dichotomy in spinal- vs prefrontal-projecting locus coeruleus modules splits descending noradrenergic analgesia from ascending aversion and anxiety in rats. Elife 6:e29808
26. Holden JE, Schwartz EJ, Proudfit HK (1999) Microinjection of morphine in the A7 catecholamine cell group produces opposing effects on nociception that are mediated by alpha1- and alpha2-adrenoceptors. Neuroscience 91:979–990
27. Howorth PW, Teschemacher AG, Pickering AE (2009) Retrograde adenoviral vector targeting of nociresponsive pontospinal noradrenergic neurons in the rat in vivo. J Comp Neurol 512:141–157
28. Imbe H, Kimura A (2016) Repeated forced swim stress affects the expression of pCREB and ΔFosB and the acetylation of histone H3 in the rostral ventromedial medulla and locus coeruleus. Brain Res Bull 127:11–22
29. Imbe H, Murakami S, Okamoto K, Iwai-Liao Y, Senba E (2004) The effects of acute and chronic restraint stress on activation of ERK in the rostral ventromedial medulla and locus coeruleus. Pain 112:361–371
30. Jennings EM, Okine BN, Roche M, Finn DP (2014) Stress-induced hyperalgesia. Prog Neurobiol 121:1–18
31. Joo J-Y, Schaukowitch K, Farbiak L, Kilaru G, Kim T-K (2016) Stimulus-specific combinatorial functionality of neuronal c-fos enhancers. Nat Neurosci 19:75–83
32. Kaushal R, Taylor BK, Jamal AB, Zhang L, Ma F, Donahue R et al (2016) GABA-A receptor activity in the noradrenergic locus coeruleus drives trigeminal neuropathic pain in the rat; contribution of NAα1 receptors in the medial prefrontal cortex. Neuroscience 334:148–159
33. Kim JJ, Shajib MS, Manocha MM, Khan WI (2012) Investigating intestinal inflammation in DSS-induced model of IBD. J Vis Exp 60:3678
34. Lackner JM, Brasel AM, Quigley BM, Keefer L, Krasner SS, Powell C et al (2010) The ties that bind: perceived social support, stress, and IBS in severely affected patients. Neurogastroenterol Motil 22:893–900
35. Laird JMA, Martinez-Caro L, Garcia-Nicas E, Cervero F (2001) A new model of visceral pain and referred hyperalgesia in the mouse. Pain 92:335–342
36. Liu L, Tsuruoka M, Maeda M, Hayashi B, Inoue T (2007) Coeruleospinal inhibition of visceral nociceptive processing in the rat spinal cord. Neurosci Lett 426:139–144
37. Liu L, Tsuruoka M, Maeda M, Hayashi B, Wang X, Inoue T (2008) Descending modulation of visceral nociceptive transmission from the locus coeruleus/subcoeruleus in the rat. Brain Res Bull 76:616–625
38. Llorca-Torralba M, Borges G, Neto F, Mico JA, Berrocoso E (2016) Noradrenergic Locus Coeruleus pathways in pain modulation. Neuroscience 338:93–113
39. Llorca-Torralba M, Camarena-Delgado C, Suárez-Pereira I, Bravo L, Mariscal P, Garcia-Partida JA et al (2022) Pain and depression comorbidity causes asymmetric plasticity in the locus coeruleus neurons. Brain 145:154–167
40. Llorca-Torralba M, Mico JA, Berrocoso E (2018) Behavioral effects of combined morphine and MK-801 administration to the locus coeruleus of a rat neuropathic pain model. Prog Neuropsychopharmacol Biol Psychiatry 84:257–266
41. Llorca-Torralba M, Suárez-Pereira I, Bravo L, Camarena-Delgado C, Garcia-Partida JA, Mico JA et al (2019) Chemogenetic silencing of the locus coeruleus-basolateral amygdala pathway abolishes pain-induced anxiety and enhanced aversive learning in rats. Biol Psychiatry 85:1021–1035
42. Martins I, Carvalho P, de Vries MG, Teixeira-Pinto A, Wilson SP, Westerink BHC et al (2015) Increased noradrenergic neurotransmission to a pain facilitatory area of the brain is implicated in facilitation of chronic pain. Anesthesiology 123:642–653
43. Mayer EA, Knight R, Mazmanian SK, Cryan JF, Tillisch K (2014) Gut microbes and the brain: paradigm shift in neuroscience. J Neurosci 34:15490–15496
44. McBurney-Lin J, Lu J, Zuo Y, Yang H (2019) Locus coeruleus-norepinephrine modulation of sensory processing and perception: a focused review. Neurosci Biobehav Rev 105:190–199
45. McCall JG, Al-Hasani R, Siuda ER, Hong DY, Norris AJ, Ford CP et al (2015) CRH engagement of the locus coeruleus noradrenergic system mediates stress-induced anxiety. Neuron 87:605–620
46. Meng XW, Budra B, Skinner K, Ohara PT, Fields HL (1997) Noradrenergic input to nociceptive modulatory neurons in the rat rostral ventromedial medulla. J Comp Neurol 377:381–391
47. Mills EP, Di Pietro F, Alshelh Z, Peck CC, Murray GM, Vickers ER et al (2018) Brainstem pain-control circuitry connectivity in chronic neuropathic pain. J Neurosci 38:465–473
48. Neubert MJ, Kincaid W, Heinricher MM (2004) Nociceptive facilitating neurons in the rostral ventromedial medulla. Pain 110:158–165
49. Olango WM, Finn DP (2014) Neurobiology of stress-induced hyperalgesia. Curr Top Behav Neurosci 20:251–280
50. Oliva V, Gregory R, Davies W-E, Harrison L, Moran R, Pickering AE et al (2021) Parallel cortical-brainstem pathways to attentional analgesia. Neuroimage 226:117548
51. Pertovaara A, Wei H, Hämäläinen MM (1996) Lidocaine in the rostroventromedial medulla and the periaqueductal gray attenuates allodynia in neuropathic rats. Neurosci Lett 218:127–130
52. Poe GR, Foote S, Eschenko O, Johansen JP, Bouret S, Aston-Jones G et al (2020) Locus coeruleus: a new look at the blue spot. Nat Rev Neurosci 21:644–659
53. Proudfit HK (1988) Pharmacologic evidence for the modulation of nociception by noradrenergic neurons. Prog Brain Res 77:357–370
54. Randich A, Mebane H, DeBerry JJ, Ness TJ (2008) Rostral ventral medulla modulation of the visceromotor reflex evoked by urinary bladder distension in female rats. J Pain 9:920–926
55. Robertson SD, Plummer NW, de Marchena J, Jensen P (2013) Developmental origins of central norepinephrine neuron diversity. Nat Neurosci 16:1016–1023
56. Saadé NE, Jabbur SJ (2008) Nociceptive behavior in animal models for peripheral neuropathy: spinal and supraspinal mechanisms. Prog Neurobiol 86:22–47
57. Sagami Y, Shimada Y, Tayama J, Nomura T, Satake M, Endo Y et al (2004) Effect of a corticotropin releasing hormone receptor antagonist on colonic sensory and motor function in patients with irritable bowel syndrome. Gut 53:958–964
58. Schwarz LA, Miyamichi K, Gao XJ, Beier KT, Weissbourd B, DeLoach KE et al (2015) Viral-genetic tracing of the input-output organization of a central noradrenaline circuit. Nature 524:88–92
59. Seo DO, Zhang ET, Piantadosi SC, Marcus DJ, Motard LE, Kan BK et al (2021) A locus coeruleus to dentate gyrus noradrenergic circuit modulates aversive contextual processing. Neuron 1091:2116–2130
60. Shanker S, Saroj N, Cordova EJ, Jarillo-Luna RA, López-Sánchez P, Terrón JA (2020) Chronic restraint stress induces serotonin transporter expression in the rat adrenal glands. Mol Cell Endocrinol 518:110935
61. Sharma Y, Xu T, Graf WM, Fobbs A, Sherwood CC, Hof PR et al (2010) Comparative anatomy of the locus coeruleus in humans and nonhuman primates. J Comp Neurol 518:963–971
62. Simrén M, Ringström G, Björnsson ES, Abrahamsson H (2004) Treatment with hypnotherapy reduces the sensory and motor component of the gastrocolonic response in irritable bowel syndrome. Psychosom Med 66:233–238
63. Singewald N, Philippu A (1998) Release of neurotransmitters in the locus coeruleus. Prog Neurobiol 56:237–267
64. Suárez-Pereira I, Llorca-Torralba M, Bravo L, Camarena-Delgado C, Soriano-Mas C, Berrocoso E (2022) The role of the locus coeruleus in pain and associated stress-related disorders. Biol Psychiatry 91:786–797
65. Suzuki R, Rahman W, Hunt SP, Dickenson AH (2004) Descending facilitatory control of mechanically evoked responses is enhanced in deep dorsal horn neurones following peripheral nerve injury. Brain Res 1019:68–76
66. Tanaka M, Matsumoto Y, Murakami T, Hisa Y, Ibata Y (1996) The origins of catecholaminergic innervation in the rostral ventromedial medulla oblongata of the rat. Neurosci Lett 207:53–56
67. Taylor BK, Westlund KN (2017) The noradrenergic locus coeruleus as a chronic pain generator. J Neurosci Res 95:1336–1346
68. Théodorou V (2013) Susceptibility to stress-induced visceral sensitivity: a bad legacy for next generations. Neurogastroenterol Motil 25:927–930
69. Totah NK, Neves RM, Panzeri S, Logothetis NK, Eschenko O (2018) The locus coeruleus is a complex and differentiated neuromodulatory system. Neuron 99:1055–1068
70. Totah NKB, Logothetis NK, Eschenko O (2019) Noradrenergic ensemble-based modulation of cognition over multiple timescales. Brain Res 1709:50–66

71. Tsuruoka M, Wang D, Tamaki J, Inoue T (2010) Descending influence from the nucleus locus coeruleus/subcoeruleus on visceral nociceptive transmission in the rat spinal cord. Neuroscience 165:1019–1024
72. Vanegas H, Schaible H-G (2004) Descending control of persistent pain: inhibitory or facilitatory? Brain Res Brain Res Rev 46:295–309
73. Vera-Portocarrero LP, Xie JY, Yie JX, Kowal J, Ossipov MH, King T et al (2006) Descending facilitation from the rostral ventromedial medulla maintains visceral pain in rats with experimental pancreatitis. Gastroenterology 130:2155–2164
74. Viisanen H, Pertovaara A (2007) Influence of peripheral nerve injury on response properties of locus coeruleus neurons and coeruleospinal antinociception in the rat. Neuroscience 146:1785–1794
75. West WL, Yeomans DC, Proudfit HK (1993) The function of noradrenergic neurons in mediating antinociception induced by electrical stimulation of the locus coeruleus in two different sources of Sprague-Dawley rats. Brain Res 626:127–135
76. Wiech K, Tracey I (2009) The influence of negative emotions on pain: behavioral effects and neural mechanisms. Neuroimage 47:987–994
77. Zhuo M (2016) Neural mechanisms underlying anxiety-chronic pain interactions. Trends Neurosci 39:136–145
78. Zhuo M, Gebhart GF (2002) Facilitation and attenuation of a visceral nociceptive reflex from the rostroventral medulla in the rat. Gastroenterology 122:1007–1019

Publisher's Note